



# Effects of Nb, V, and W on Microstructure and Abrasion Resistance of Fe-Cr-C Hardfacing Alloys

*Various alloying elements were added to a self-shielded flux cored welding wire to determine their influence on the formation of wear-resistant weld metal*

BY QINGBAO WANG AND XIAOYAN LI

## ABSTRACT

The morphology of Nb, V, and W in Fe-Cr-C hardfacing alloy microstructure has been investigated with optical microscope (OP) and scanning electron microscope (SEM). The strengthening mechanism of the three alloying elements in the cladding metal has been analyzed. The causes for different hardnesses and abrasion resistances have been studied. The following is exhibited from the experiment: 1) with addition of around 6% Nb, the hardness and wear resistance of the cladding metal increased; 2) with a small addition of V and W, the hardness increased and the wear resistance improved more noticeably; and 3) with a further slight increase in the content content of V and W, the hardness of the cladding metal increased in some sort, but had no further significant effect on the wear resistance. The optimization of the alloying elements is required to obtain good wear resistance and economic efficiency by strengthening matrix and carbides simultaneously.

## Introduction

Thanks to their high volume fraction of hard carbide fibers, Fe-Cr-C hardfacing alloys are used extensively in the mining and mineral processing industries where high wear and abrasion resistance are required. By depositing self-shielding flux cored welding wire, cladding metal with high-chromium content (up to 30%) and carbon content (up to 6%) can be obtained. Water cooling during welding will promote the formation of monocrystalline  $M_7C_3$  (where M represents the alloying element) carbide rods of irregular hexagonal cross section in a metastable matrix of austenite. These  $M_7C_3$  carbide rods play an important role in improving the wear resistance of the material. Modern Fe-Cr-C wear-resistant material has been studied based on tough austenite matrix with dispersion of hard carbide particles. In this investigation, the alloying elements of Nb, V, and W were added and varied in a self-shielded flux cored welding wire to deter-

mine the influence of the alloying elements on the formation of abrasion-resistant skeletal carbide particles and the matrix (austenite and its transformation product). The abrasive testing result is discussed with the intention to provide a theoretical foundation for future investigations and applications of the Fe-Cr-C wear-resistant material (Refs. 1-9).

## Experimental Methods and Procedures

### Selection of Alloying System

From the Fe-Cr-C phase diagrams

## KEYWORDS

Fe-Cr-C Hardfacing Alloy  
Abrasion Resistance  
Wear-Resistant Carbides  
Alloying Elements  
Self-Shielded Flux Cored  
Welding Wire

(Figs. 1, 2) (Refs. 10, 11), it is known that in order to obtain sufficient wear-resistant fibers — primary  $M_7C_3$  carbides — C content should be more than 4.2% and Cr content more than 10%.

High C content will lead to the formation of primary chromium carbide, which will consume the Cr content in the matrix. The reduction of Cr content will in turn weaken the matrix's hardenability and corrosion resistance. To overcome this weakness, the content of Cr shall be increased. It is pointed out that increasing Cr content in the high-chromium white iron can reduce the eutectic carbon content (Ref. 12). For example, the alloys with Cr concentrations of 5, 13, 17, and 25% have carbon contents of 4.0, 3.7, 3.5, and 3%, respectively, at the eutectic point. In other words, increasing the Cr content and without changing the C content will shift the eutectic point to the left, and more chromium carbides will be formed. Thus, it is not necessary to increase the C content to get more chromium carbide, and therefore the toughness of the deposited weld metal will not be compromised (Ref. 12).

In this experiment, the welding deposit of the Fe-Cr-C self-shielded flux-cored welding wire has been designed as 4.7% C and 23% Cr, which is a common commercial embodiment of a primary chromium carbide hardfacing alloy. It can be seen from Fig. 2 that with these chemical compositions, it is easy to form sufficient hard primary  $M_7C_3$  fiber at high temperature.

The welding wire was made of  $0.3 \times 17$  mm steel strip with extra-low carbon. The diameter of the wire was 3.2 mm and the weight proportion was  $50 \pm 1.5\%$ .

With the same contents of C and Cr in the welding deposit, the microstructures and mechanical properties of the cladding metal were investigated by adding different amounts of alloying ele-

Q. WANG is with MCC Welding Science & Technology Co. Ltd., and X. LI (xiaoyan@sasglobalcorp.com) is with SAS Global Corp., Warren, Mich.

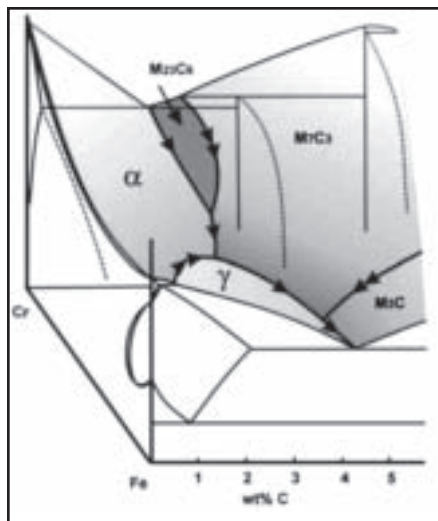
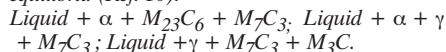


Fig. 1 — Metastable Fe-Cr-C phase diagram for carbon contents less than 5%. The bold black lines are the monovariant lines separating the primary solidification fields. Conventionally, eutectic-type equilibria are indicated by a single arrow and those of peritectic type by a double arrow. The dotted lines represent the limiting solid compositions in equilibrium with the liquid on the corresponding monovariant line. There are three four-phase invariant equilibria (Ref. 10):



ments of Nb, V, and W.

It is known that additional alloying of high-chromium cast irons with carbide-forming elements (Nb, V, Mo, W, etc.) significantly affects the mechanical properties, chemical compositions, and dispersion of the carbide phases, as well as the strength of the matrix (martensite, austenite). Based on the previous experiment and research, in this experiment the Nb concentration started with 6%.

The welds were deposited in six layers

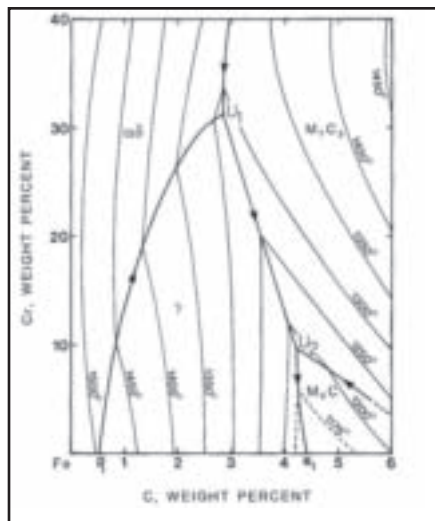


Fig. 2 — Fe-rich corner of metastable C-Cr-Fe liquidus surface (Ref. 11).

so that the top layer could be examined in an undiluted condition. Five welding beads were put on each layer and the overlapping width was 30% of the welding bead. Water cooling was applied during the welding process and the interpass temperature was controlled below 200°C. The detailed welding parameters are shown in Table 1. Chemical compositions of the welding deposit were analyzed, as shown in Table 2. Sample 1 is a Fe-Cr-C alloy without adding any other alloying elements and is used as the reference sample. Sample 2 add 6.12% Nb on the basis of Sample 1. Sample 3 adds a small quantity of V and W on the basis of Sample 2. Sample 4 adds a comparatively large quantity of V and W on the basis of Sample 2.

## Experimental Procedures

Microstructures of the welding deposit were observed with the Neophot 21 microscope. The samples were also examined by using a scanning electron microscope (JSM-6301F).

The macrohardness of the welding deposit samples was measured with an H-100 Rockwell hardness machine (1470 kN load). Nine measurements were made on each sample, with the highest and the lowest values omitted, and an average of the remaining seven numbers was calculated and recorded. The microhardness of the welding deposit was measured (on both carbides and matrix) with an HXD-1000 Vickers hardness machine (0.98 N load).

Abrasion-resistant tests were performed on a MLS-225 wet sand rubber wheel AR testing machine, according to the procedure ASTM G105. The specimen size was 57.9 × 25.4 × 11 mm. After the specimen was cut, it was ground using No. 600 SiC paper to remove the rough surface layer then polished so that the testing surface was parallel to the base surface. The rotating speed of the rubber wheel was 245 rev/min, its diameter was 178 mm, and the hardness was 60 HA (Shore hardness). Wet sand was made of 1-kg water and 1.5-kg abrasion SiO<sub>2</sub> round sand (50~70 mesh). The applied load was 10 kg. The total revolution of the rubber wheel was 1000. Before and after each test, the specimen was ultrasonically cleaned in acetone, blown dry with warm air, and then weighed to determine the weight loss by using an electronic balance that has an accuracy of 0.1 mg. The working theory of the testing machine is shown in Fig. 3. The abrasion testing equipment is shown in Fig. 4.

The wear resistance of Sample No. 1 is set as 1. Other samples are compared with

Table 1 — Welding Parameters

Welding Current I/A	Welding Voltage U/V	Welding Speed v/(mm.s <sup>-1</sup> )	Stick out l/mm	Interpass Temperature t/°C	Welding Wire Diameter (Φ/mm)	Depositing Numbers
480~520A	34~38 V	800~850 mm/min	20~35mm	<200°C	3.2	6 Layers 5 Beads

Table 2 — Chemical Compositions of Experimental Samples (wt-%)

Samples	Chemical Composition (%)					
	C	Cr	Nb	V	W	Mn+Si
Sample 1	4.74	23.56	0	0	0	<0.2
Sample 2	4.81	22.98	6.12	0	0	<0.2
Sample 3	4.72	23.72	6.03	0.21	0.23	<0.2
Sample 4	4.69	22.57	6.21	0.39	0.42	<0.2

Sample 1 is a Fe-Cr-C alloy without adding any other alloying elements and is used as the reference sample. Sample 2 adds 6.12% Nb on the basis of Sample 1. Sample 3 adds a small quantity of V and W on the basis of Sample 2. Sample 4 adds a comparatively large quantity of V and W on the basis of Sample 2.

Sample 1 and get a relative wear resistance coefficient  $\epsilon$  ( $\epsilon$  = weight loss of Sample No. 1: weight loss of other sample). The larger the value of  $\epsilon$ , the more wear resistant is the sample. Five testing specimens were made from each sample and were tested separately. The highest and the lowest weight loss numbers were omitted, and an average of the remaining three numbers was calculated and recorded.

## Results and Discussion

### Morphology of Nb, V, and W under Optical Microscope

It is stated by G. Powell (Ref. 8) that in a Fe-Cr-C alloy with hypereutectic compositions, the as-solidified microstructure is one of long parallel aligned primary carbides in a eutectic matrix of carbide rods in austenite, or short randomly orientated primary carbides in a eutectic matrix.

In this experiment, metallographic specimens were prepared for Samples 1–4. The specimens were ground, polished, and etched by Picral-Nital solution. The specimens were examined using Neophot 21 microscopy. The microstructures are shown in Fig. 5.

It is shown that all of the four samples have a typical hypereutectic microstructure, which consists of hypereutectic (primary)  $M_7C_3$  and matrix. The matrix is composed of mainly austenite and some ledeburite transformed from austenite. There is a large quantity of monocrystalline  $M_7C_3$  fibers, which have a hexagonal cross section consistent with the pseudo hexagonal crystal structure of  $M_7C_3$  carbide. The primary  $M_7C_3$  carbide is the first phase to form on cooling. The residual liquid then decomposes into austenite and more fine  $M_7C_3$  carbide.

Figure 5A is for Sample No. 1. The microstructure is described as above. The characteristic of this material is hypereutectic microstructure with hard  $M_7C_3$  primary chromium carbides dispersed in a tough austenitic matrix.

Figure 5B shows that other than the white carbide, there are some light gray alloy carbides. Those carbides are formed clustering with chromium carbide or dispersing separately in the matrix. It is defined by SEM (Fig. 6B) that those carbides are niobium carbides.

Niobium has a strong affinity for carbon and nitrogen, and easily forms niobium carbide with carbon. In hypereutectic high-chrome cast iron, Nb exists mainly as niobium carbides. At 1300°C, niobium carbide starts to form, which is called primary carbide. With the formation of NbC, there are zones enriched with Fe and Cr, which raise the austenite formation temperature. The Cr and C surrounding NbC work as the nu-

clei to form austenite. Since the partition ratio of Cr and C in  $\gamma$ -Fe is smaller than 1, C and Cr will be expelled to the surrounding area during the formation of austenite. Thus, the area between NbC and austenite will have an enrichment of Cr and C. During the rapid cooling after welding, there is no sufficient time for Cr and C to diffuse, which creates a propitious condition for the nucleus formation of chromium carbide. The nucleus formation occurs on NbC or the surrounding area, and then chromium carbide forms from the nuclei. Therefore, niobium carbide and chromium carbide often cluster together.

Figure 5C and D shows the microstructure of Samples 3 and 4. It is noticed that those microstructures look similar to that of Sample 2, except that Samples 3 and 4 have some scattered and fine carbides present in the matrix due to the fact that V and W were added.

### The Morphology of Nb, V, and W under SEM

Figure 6 shows the SEM-EDS compositional maps of the deposits of Samples 2, 3, and 4, in which it is possible to identify the carbide types present in the microstructures. The SEM-EDS (electron dispersive spectrograph) images show the distribution of the elements of Nb, V, and W.

The element Nb is usually agglomerated and connected with the chromium carbide particles. At high Nb content (e.g., 6%), niobium carbide directly precipitates at higher temperature in the melt before the solidification of the alloy starts. By this way the NbC could develop an exact crystallographic cubic form, as Fig. 6B shows. It can be seen from Fig. 6B and F that the cubic niobium carbides are randomly distributed in the structure. Niobium formed cubic niobium carbides directly and strengthened the cladding metal.

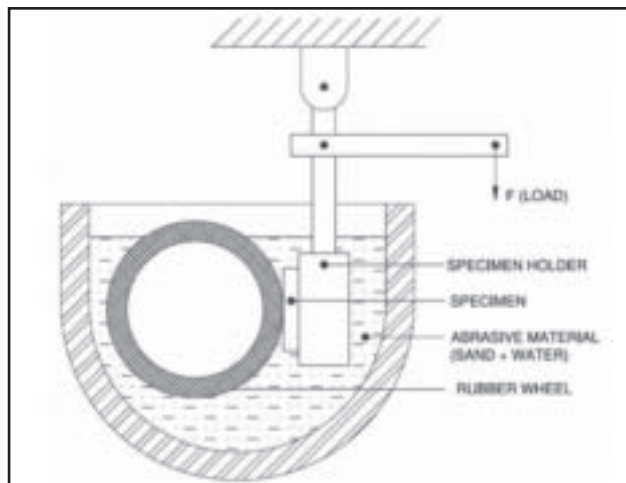


Fig 3 — Schematic drawing for the abrasion test.



Fig. 4 — Abrasion test equipment (MLS-225 wet sand rubber wheel test machine).

It is seen from Fig. 6H that V exists in three forms: 1) some solved in the matrix; 2) some solved in the primary and eutectic carbides; and 3) the others (in a small amount) formed fine carbides with W and Cr. Therefore, V can strengthen the matrix and the carbides, and in the meanwhile it can form the primary carbides directly.

There are three formations of W, which include: 1) dispersion in the matrix; 2) dispersion on the carbides, where it has strong ability to form primary carbide with Nb, which can be seen from Fig. 6F and G; and 3) the formation of fine carbides with V and Cr. Tungsten not only reinforces the matrix and carbide, but also forms skele-

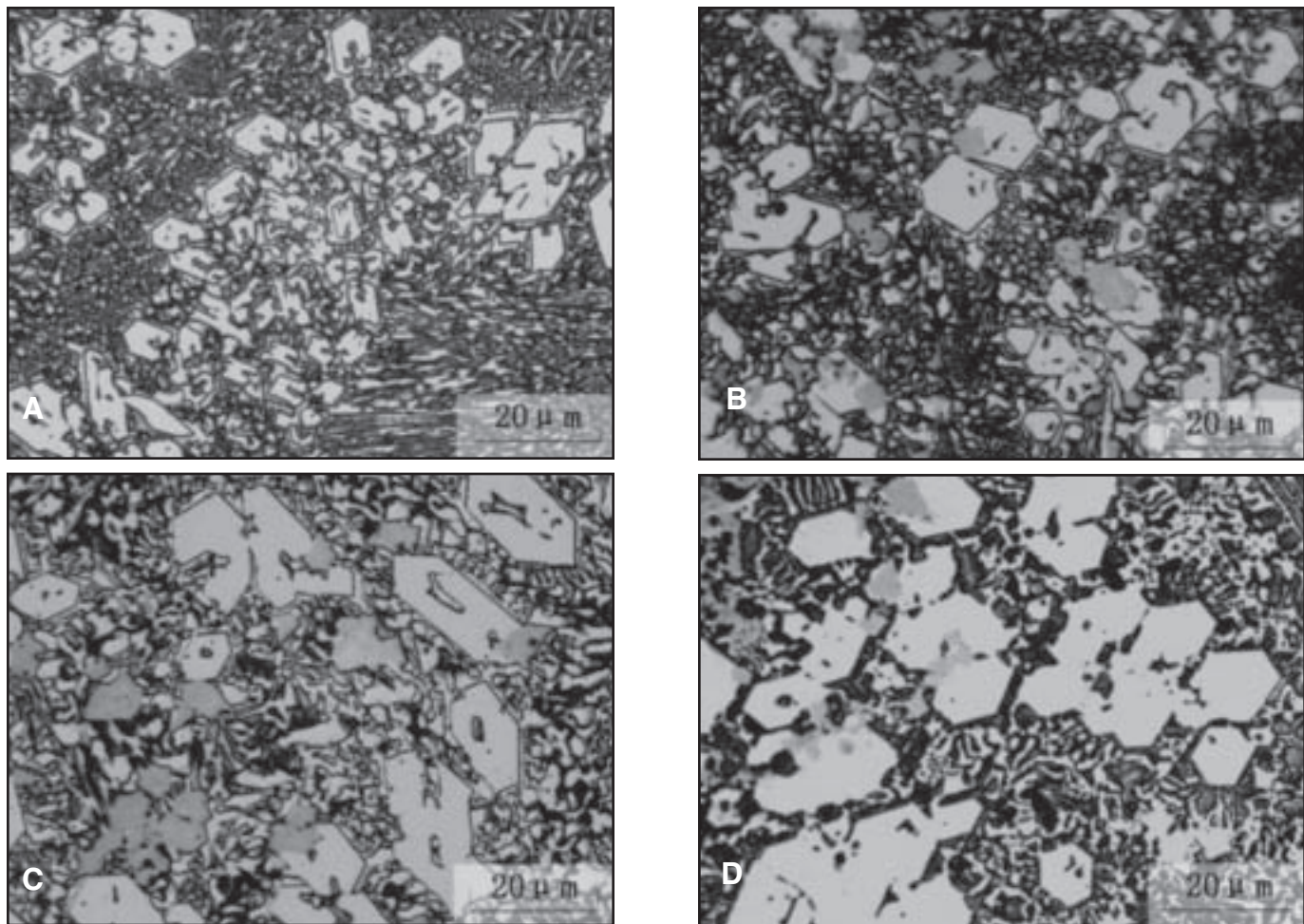


Fig. 5 — Microstructures of four samples and the etchant is Picral+Nital solution. A — Sample No. 1; B — Sample No. 2; C — Sample No. 3; D — Sample No. 4.

tal primary carbide, which is the main force to fight abrasion.

The matrix surrounding the large primary particles was analyzed by SEM and the energy spectrum analysis. It is shown from Fig. 6C, D, I, and J that in both Samples 2 and 4, it is always Fe-rich and Cr-

lean around the primary carbides.

In Sample 2, the formation of primary carbide consumes C and Cr, and during the fast cooling, there is no sufficient time for C and Cr in the austenite to migrate; hence, a low-Cr, low, C austenite transformation zone was formed surrounding the

primary carbide. The hardness of this layer is measured by HXD-1000 as HV<sub>360</sub>.

In Sample 4, with the addition of V and W, the eutectic point of Fe-C diagram drifted to the left. The carbon content in the austenite matrix decreased and thus the amount of the carbides increased. With the increasing quantity of carbides, the growth of austenite dendrite was hindered, and therefore, a finer austenite matrix was formed. There existed carbonitride of V and W in the iron liquid between the austenite dendrites, which worked as the nuclei during the solidification. That is why there formed a substantial amount of fine carbide in the austenite matrix.

Table 3 — Energy Spectrum Analysis of Sample 4

	Alloying Element (wt-%)				
	C	V	Cr	Fe	W
A Fine primary carbide	21.01	0.53	24.89	51.91	1.67
B Blade-like carbide	14.97	0.12	6.64	76.59	1.86

Table 4 — Hardness and Relative Wear Resistance of Samples 1–4

No.	Weight Loss of 3 Specimens after 1000 Revolutions (mg)			Average Weight Loss (mg)	Relative Wear Resistance Ratio $\epsilon$	Hardness (HRC)
Sample 1	171.3	189.3	178.5	179.7	1	61.2
Sample 2	132.9	118.3	134.0	128.4	1.40	62.8
Sample 3	96.5	110.3	98.6	101.8	1.77	63.6
Sample 4	102.7	99.5	94.5	98.9	1.82	64.1

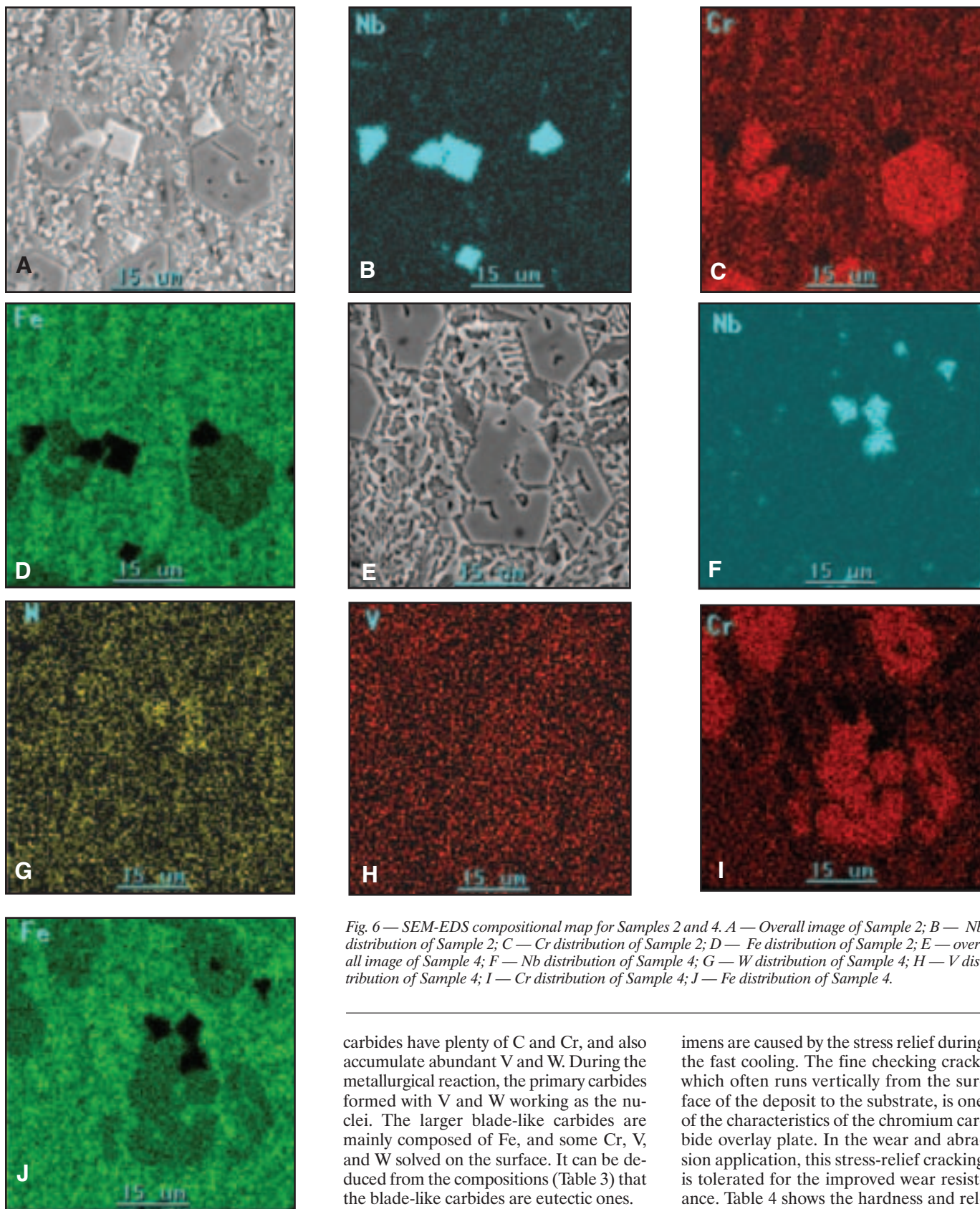


Fig. 6 — SEM-EDS compositional map for Samples 2 and 4. A — Overall image of Sample 2; B — Nb distribution of Sample 2; C — Cr distribution of Sample 2; D — Fe distribution of Sample 2; E — overall image of Sample 4; F — Nb distribution of Sample 4; G — W distribution of Sample 4; H — V distribution of Sample 4; I — Cr distribution of Sample 4; J — Fe distribution of Sample 4.

carbides have plenty of C and Cr, and also accumulate abundant V and W. During the metallurgical reaction, the primary carbides formed with V and W working as the nuclei. The larger blade-like carbides are mainly composed of Fe, and some Cr, V, and W solved on the surface. It can be deduced from the compositions (Table 3) that the blade-like carbides are eutectic ones.

#### The Effects of Nb, V, and W on Hardness and Wear Resistance

Figure 8 shows the surface morphology of Samples 1, 2, and 3 after the abrasion test. The fine checking cracks on the spec-

imens are caused by the stress relief during the fast cooling. The fine checking crack, which often runs vertically from the surface of the deposit to the substrate, is one of the characteristics of the chromium carbide overlay plate. In the wear and abrasion application, this stress-relief cracking is tolerated for the improved wear resistance. Table 4 shows the hardness and relative wear resistance of Sample 1–4.

#### The Effect of Nb, V, and W on Hardness

The basic factors that decide the macro-hardness of Fe-Cr-C hardfacing alloy include the matrix microstructure and the

From Table 3 and Fig. 7 (both for the energy spectrum analysis of Sample 4), it can be seen that around the large hexagonal primary carbide, there exist two forms of carbides: fine primary carbides and larger blade-like carbides. The isolated fine

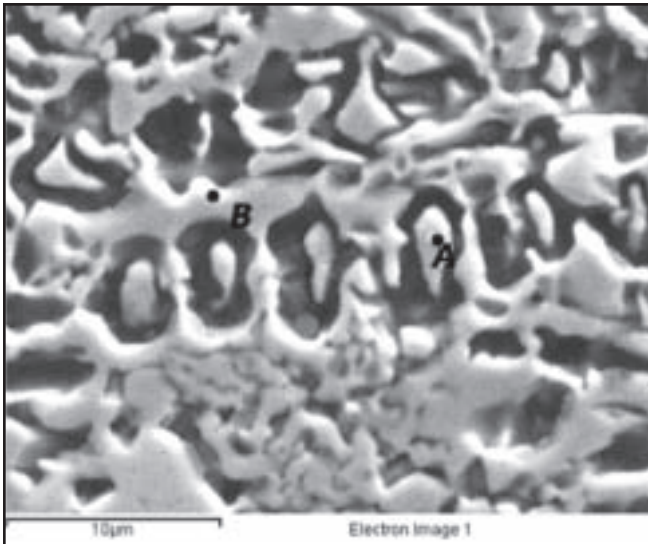


Fig 7 — SEM image of the matrix around the large primary carbide (Sample 4): (A) fine primary carbides and (B) larger blade-like carbides.

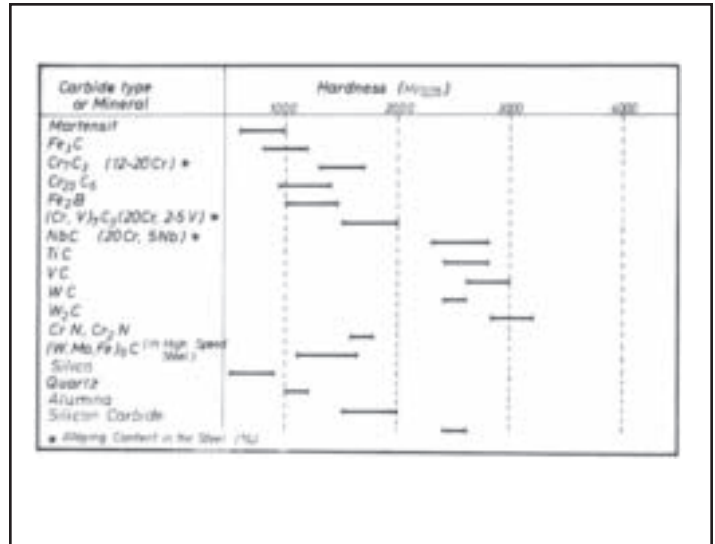


Fig. 9 — Hardness of various carbides and other hard substances (Ref. 13).

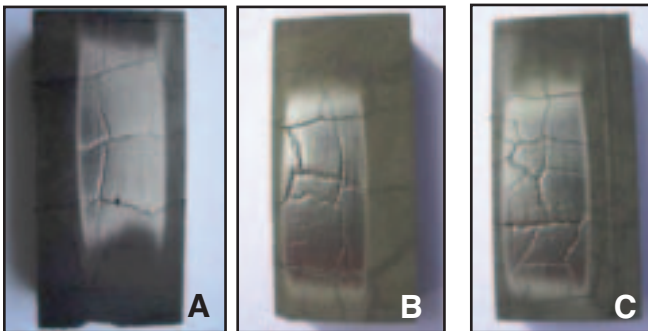


Fig. 8 — Abrasion surface morphology of Samples 1, 2, and 3 after the abrasion test. A — Sample 1; B — Sample 2; C — Sample 3.

volume fraction of hard carbide particles. The most important factor that affects the austenite formation and the volume fraction of carbide is the carbon content.

In this experiment, there is little difference in the carbon content for the four samples. The matrix microstructures look similar and the volume fractions of the carbide are about the same for all samples. For general reference, the microhardness for various carbides and other hard substances is shown in Fig. 9.

In this study, the carbides in the microstructure were big enough to measure the microhardness with a load of 0.98 N. In the Nb-, V-, and W-free alloy Sample 1 (4.74C-23.56Cr), the chromium carbides had an average hardness of 1410 HV with a standard deviation of 220 HV. In Sample 2 (4.81C-22.98Cr-6.12 Nb), the chromium carbides were harder. An average value of 1520 HV was found. In Sample 3 (4.72C-23.72Cr-6.03Nb-0.21V-0.23W), the average microhardness of carbides was 1590 HV and in Sample 4 (4.69C-22.57Cr-6.21Nb-0.39V-0.42W) was 1610 HV.

average hardness of 1410 HV, which means that the chromium carbide is not alloyed with Nb. The niobium in the melts has been bound in the NbC.

In Samples 3 and 4, fortifying elements V and W were added. Microhardness tests showed that the added V and W were dissolved in chromium carbide and increased the hardness of the  $M_7C_3$  carbides by solid-solution hardening. Vanadium and W dispersed in the matrix and carbides, thus reinforcing the matrix and eutectic carbide simultaneously. Vanadium and W also agglomerate and form primary carbides. Therefore, the cladding metal with addition of V and W was harder than Sample 2. With the increase of V and W, the extent of reinforcement increased. But in Table 4, it does not show a considerable macrohardness increase from Sample 3 to Sample 4. The main reason is probably that V and W are strong elements in forming carbides, and consume more carbon, which probably leads to the reduction of carbon content in the matrix and, therefore, the hardness of the matrix. High

hardness requires a combination of fortified carbides and reinforced matrix, as stated by Askeland (Ref. 14), “The strength of a fiber-reinforced composite depends on both the strength of the raw fiber and bonding between the fibers and the matrix.”

#### The Effect of Nb, V, and W on Wear Resistance

Comparing the relative wear resistance in Table 4, it is found that Sample 1 without any addition of alloying elements has the most inferior wear resistance. Sample 2 with the addition of 6% Nb has a relative wear resistance coefficient of 1.40 compared to Sample 1, and the coefficient of Sample 3 is 1.77, while Sample 4 with higher quantity of V and W has a relative wear resistance coefficient of 1.82.

Sample 2 has a good wear resistance because of the formation of hard primary niobium carbide NbC. The coarse  $M_7C_3$  carbide particles provided a barrier against microgouging and microcutting. This beneficial effect is reinforced by the NbC particles, which prevent the detachment of  $M_7C_3$  carbides due to their finely dispersed distribution in the matrix, as shown by Chen and Chang (Ref. 15). The experimental result shows that the wear resistance of Sample 2 is 1.4 times better than Sample 1. Sample 3 adds matrix-fortifying elements V and W, which not only fortifies the matrix but also the carbide, thus a good combination of hard carbides and tough matrix is obtained. The experimental result shows that the wear resistance of Sample 3 is 1.26 times better than Sample 2. Sample 4 adds slightly more V and W, which leads to formation of more vanadium and tungsten carbides. But the formation of these vanadium and tungsten

carbides reduces the carbon content and hardness in the matrix. In this experiment, adding slightly more V and W did not get a good combination of hard carbides and tough matrix, therefore the wear resistance of Sample 4 did not improve much, compared to Sample 3. The experimental result shows that the wear resistance of Sample 4 is 1.02 times of Sample 3.

The erosive weight loss of high-chromium white irons is a combination of the weight loss due to matrix removal and carbide removal. Large quantity of carbides shortens the distance between each carbide particle, and reduces the area of matrix between them. Hence the matrix can be protected well. On the other hand, the matrix can in turn support the primary and secondary carbides. The key is to obtain a good combination of tough matrix and hard carbide particles. In high-chrome cast iron, in order to obtain good wear resistance, it is required to optimize the alloying elements so that both the matrix and carbide will be reinforced.

## Conclusions

1) With the addition of around 6% Nb in the cladding metal, the hardness increases and the wear resistance increases. With the slight addition of W and V in the cladding metal, the hardness increases to

some extent and the wear resistance increases. With a further slight addition of W and V, the hardness increases further, but there is not much difference in wear resistance.

2) In the cladding metal, Nb increases the hardness of carbides by forming primary carbide, while V and W reinforce both matrix and carbides, and also form primary carbides.

3) In order to obtain good wear resistance, it is required to optimize the alloying elements and get a good combination of hard carbides and tough matrix.

## References

1. Svensson, L. E., Grefot, B., Ulander, B., and Bhadeshia, H.K.D.H. 1986. Fe-Cr-C hardfacing alloys for high-temperature applications. *Journal of Material Science*, Vol. 21, pp. 1015–1019.
2. Hao, S. 1992. *High Carbon Wear Resistance Casting*, Coal Industry Publishing House, Beijing, pp. 79–180, pp. 230–232.
3. Atamert, S., and Bhadeshia, H. K. D. H. 1990. Microstructure and stability of Fe-Cr-C hardfacing alloys. *Materials Science and Engineering*, Vol. A130, pp. 101–112.
4. Sharma, T, Maria, S., and Dwiedi, D. K. 2005. Abrasive wear behavior of Fe-30Cr-3.6C overlays deposited on mild steel. *ISIJ International*, 45(9): 1322–1325.
5. Powell, G. 1997. The effect of Si on the relationship between orientation and carbide

morphology in high chromium white irons. *Journal of Materials Science* 32, pp. 561–565.

6. Wo, W., and Wu, L. T. 1996. The wear behavior between hardfacing materials. *Metallurgical Material Transaction*, A 27A, pp. 3639–3648.

7. Choteborsky, R. 2008. Abrasive wear of high chromium Fe-Cr-C hardfacing alloys. *Res. Agr. Eng.*, pp. 192–198

8. Powell, G. L. F., Brown, I. H., and Nelson, G. D. *Tough Hypereutectic High Chromium White Iron — A Double In-Situ Fibrous Composite*. The University of Adelaide, South Australia.

9. Sun, D., and Wang, W., et al. 2003. Effects of alloying elements on microstructure and erosion resistance of Fe-Cr weld surfacing layer, *Journal of Material and Science Technology*, 19(4): 351–354.

10. Durand-Charre, M. 2004. *The Microstructure of Steels and Cast Irons*, pp. 52–73

11. Thorpe, W. R., and Chicco, B. 1985. The Fe-rich corner of the metastable C-Cr-Fe liquidus surface. *Metallurgical Transactions A*, Vol. 16A.

12. Ju, C. 1999. *High Chromium Cast Iron and Its Application*. Metallurgical Industry Publishing House, pp. 10–20

13. Theisen, W. 1998. *Hartphasen, in Hartlegierungen und Hartverbundstoffe*, Hrsg. Hans Berns. Springer-Verlag Berlin, S. 28.

14. Askeland, D. R. 1996. *The Science and Engineering of Materials*, Third S.I. Edition, Chapman and Hall, London, p. 560.

15. Chen, H. X., and Chang, Z. C. 1993. Effect of niobium on wear resistance of 14% Cr with cast iron. *Wear* 166, pp. 197–201.

## Good News:

I'm glad to announce that peer review of research papers is now managed through an online system using Editorial Manager software. Papers can be submitted into the system directly from the *Welding Journal* page on the AWS Web site by clicking on "submit papers." You can also access the new site directly at [www.editorialmanager.com/wj/](http://www.editorialmanager.com/wj/). Follow the instructions to register or login, and make sure your information is up to date. This online system will streamline the review process, and make it easier for authors to submit papers and track their progress. If you have any questions or encounter problems, please click on "help" or "contact us" in the main navigation bar.

Best Regards,

Andrew Cullison  
Publisher  
*Welding Journal*